Structural and electronic effects of Sr substitution for Ba in $Y(Ba_{1-x}Sr_x)_2Cu_3O_w$ at varying w

F. Licci,* A. Gauzzi, and M. Marezio
Istituto Materiali Speciali per Elettronica e Magnetismo del Consiglio Nazionale delle Ricerche, Via Chiavari 18/A, 43100 Parma, Italy

G. P. Radaelli
ISIS Facility, Rutherford Appleton Laboratory, Chilton, Didcot, Oxon OX11 OQX, United Kingdom

R. Masini
Istituto per la Tecnologia dei Materiali e Processi Energetici del Consiglio Nazionale delle Ricerche, Via R. Cozzi, 53, 20125 Milano, Italy

C. Chaillout-Bougerol
Laboratoire de Cristallographie, Centre National de la Recherche Scientifique, Université Joseph Fourier, Boîte Postale 166, 38042 Grenoble Cedex 9, France

(Received 20 July 1998)

To unveil the structural mechanisms associated with T_c variations induced by either mechanical or chemical pressure, samples of the $Y(Ba_{1-x}Sr_x)_2Cu_3O_w$ system with $x \leqslant 0,0.02,0.1,0.25,0.35,0.5,0.625,0.75,1$, as well as those with $x=0.5$ and $w=6.685,6.80,6.96,6.98$, have been prepared and characterized. Characterization includes crystal structural refinements based on powder neutron diffraction data taken at room temperature, electron microscopy for detecting a possible Ba/Sr ordering, and resistive and magnetic measurements of the superconducting transition. The effects of Sr substitution on the structural parameters are equivalent to those of a pressure of approximately 10 GPa/x. The main difference is the thickness of the superconducting block CuO_2-Y-CuO_2, which increases with increasing x and decreases with increasing pressure. As a consequence of the displacement of O4 from the $(0,\frac{1}{2},0)$ to the $(x,\frac{1}{2},0)$ position, the Ba/Sr-O4 distance decreases with increasing Sr content. At constant w, T_c decreases at the rate of 20 K/x. For $x>0$, the maximum of T_c occurs at a value of w higher than for $x=0$. For $x=0.5$ the thickness of the superconducting block increases with increasing w and consequently with increasing T_c. This indicates that, at least in this system, the thickness of the superconducting block is not the key parameter controlling T_c. The stress of the Ba/Sr and the Y sites, estimated from the bond valence sums (BVSs), decreases with increasing x. For $x=0.5$, the BVS values are almost equal to the formal values of 2+ and 3+, respectively. The average BVS of Cu1 and Cu2 increases with increasing x. However, this does not correspond to a real increase because the total charge of the Cu cations, as determined by iodometric titration or neutron diffraction, remains constant with x. Our analysis of the structural data suggests that the relaxation of the Ba/Sr layer hinders the charge transfer from Cu1 to Cu2, which accounts for the decrease of T_c with increasing x. [S0163-1829(98)05645-8]

I. INTRODUCTION

In general, the application of mechanical pressure on layered cuprates increases T_c at rates that depend on the chemical composition of each specific phase. In the case of $YBa_2Cu_3O_w$ (YBCO-123), values of dT_c/dP ranging from 4–7 to 0–1 K/GPa have been reported for $w \approx 6.6$ and $w>6.9$, respectively.[1] Structural refinements of $YBa_2Cu_3O_w$ with $w=6.93$ and 6.6, as a function of pressure between 1 atm and 0.578 GPa, indicated that pressure-induced structural changes occur around the Cu2-apical oxygen bond.[2] However, it was not possible to relate these structural changes to significant variations in the charge transfer induced by pressure. Other experiments were carried out by applying pressure to $YBa_2Cu_3O_w$ (Ref. 3) at different temperatures. They allowed the authors to separate two pressure-induced effects, one due to the chain oxygen ordering and the other to variations of the structural and electronic parameters. In $YBa_2Cu_3O_{6.7}$, dT_c/dP values of 4.1 and 7.4 K/GPa have been reported for the oxygen ordering and the variation of the intrinsic parameters, respectively.

Reproduction by chemical substitutions of the structural changes induced by mechanical pressure is considered an interesting tool for engineering increases of T_c. The most direct method for reducing the interatomic distances without altering the valence balance is substituting Sr for Ba. The latter has an ionic radius smaller than the former and both are divalent. Thus the introduction of Sr would not alter the hole concentration of the CuO_2 layers. However, the introduction of Sr in $Y(Ba_{1-x}Sr_x)_2Cu_3O_w$ induces a decrease of T_c and ultimately makes the 123 phase unstable. Single-phase samples were obtained at ambient pressure up to $x \leqslant 0.5$.[4–7] The results reported by Oda *et al.*[8] on the synthesis of $YSr_2Cu_3O_w$ ($x=1$) have not been reproduced. To obtain this phase it is necessary either to carry out the synthesis under high pressure[9] or to introduce a second substituent Me on the Cu1 site and synthesize samples such as $YSr_2(Cu2)_2(Cu1)_{1-y}Me_yO_w$.[10]

Similar behavior has been observed for the Hg-based cuprates $HgBa_2Ca_{n-1}Cu_nO_{2+2n+\delta}$. If Sr is substituted for

some of the Ba cations, T_c decreases[11] and the synthesis of single-phase materials necessitates the use of either high pressure[12] or a second substituent with a valence greater than 2 on the Hg site.[13] The lattice parameters of Sr-123 and Sr-Hg12$(n-1)n$ decrease with respect to those of unsubstituted materials in a way similar to that observed by applying external pressure.[14] The introduction of Sr induces similar decreases of T_c in compounds as different as 123 and Hg-based ones; it would then be interesting to study these structures in detail in order to elucidate the structural mechanisms associated with the decreases of T_c. Veal *et al.*[5] reported, albeit incompletely, structural data for the $Y(Ba_{1-x}Sr_x)_2Cu_3O_w$ system. Other authors reported structural refinements of compounds with a second substituent on the Cu1 sites, such as Cr,[15] Re, Mo, and W.[16] However, the second substitution modifies significantly the original structure.

In order to understand the difference between the effects induced by chemical substitutions and those induced by applying mechanical pressure, we synthesized and characterized samples of $Y(Ba_{1-x}Sr_x)_2Cu_3O_w$. The structural refinements based on powder neutron diffraction data were carried out as a function of x and, for $x=0.5$, as a function of w. The electric and magnetic properties have also been measured and correlated with the structural parameters and oxygen content. It seems that the Ba cations play an important role in the high T_c of YBCO. Its substitution with a smaller cation corresponds to the application of a chemical pressure, but other important crystallographic features also change with substitution and these changes seem to play a negative role on T_c.

II. EXPERIMENT

A. Sample preparation

Samples of $Y(Ba_{1-x}Sr_x)_2Cu_3O_w$ (with nominal $x=0,0.02,0.1,0.25,0.35,0.5,0.625,0.75,1$) were prepared by a solid-state reaction of stoichiometric mixtures of Y_2O_3 (99.999%), CuO (99.99%), $BaCO_3$ (99.99%), and $SrCO_3$ (99.99%). In a few experiments ($x=0.75$ and 1) SrO_2 was also used, but no significant improvements in the system reactivity were obtained. Reagents were mixed and ground under acetone in agate mortars. The syntheses were carried out in Al_2O_3 crucibles, in air at 950 °C for a total of 80–100 h, with several intermediate coolings and grindings. Reactions were stopped when x-ray diffractograms did not reveal any difference after two consecutive treatments. Pellets 700 mg in weight and 1 cm in diameter, obtained by pressing the powders, were sintered in air at 950 °C overnight and cooled at a rate of 100 °C/h down to room temperature (*R* samples). Different annealing treatments were applied for varying the oxygen stoichiometry w. For the *A* samples, *R* pellets were heated in flowing oxygen at 880 °C for 2 h, cooled at 30 °C/h down to 480 °C, and maintained at this temperature for 50–100 h before being cooled down to room temperature. For the *S* samples, a few *A* pellets were put in a quartz ampoule together with a 1-g pellet of SrO_2. The ampoule (1 cm in diameter, 10 cm long, 2–3 mm thick) was evacuated to 10^{-5} torr, sealed, and heated up to 600 °C for 2 h in order to decompose SrO_2 and produce oxygen with a pressure of about 20–30 atm. The system was cooled down to 500 °C, maintained at this temperature for 10 h, and then cooled to room temperature. For the *G* samples a few *R* pellets were sealed in a Pyrex ampoule together with a zirconium foil 2.5 cm high and of varying lengths. The ampoules were evacuated down to 10^{-5} torr, heated to 440 °C, maintained at this temperature for 50–100 h, and cooled down to room temperature. For a fixed ampoule volume and annealing temperature, oxygen was gettered by Zr in amounts proportional to the Zr surface, the number of pellets, and the duration of annealing. Details of the procedure are given in Ref. 17.

B. Characterization

The phase analysis and structural parameters were determined by x-ray diffraction. Patterns were recorded with a D500 Siemens diffractometer, using Cu $K\alpha$ radiation. Cation stoichiometry in single-phase materials was assumed coincident with the nominal one.

Oxygen stoichiometry was determined by iodometric titration with an amperometric dead-stop end point.[18] For each composition six to eight tests were carried out. The reproducibility of results was within 0.02 ml (titrant volume), thus resulting in a precision of about 0.005 oxygen/f.u.

Electric resistivity and magnetic susceptibility were measured as a function of temperature between 300 and 4.2 K. ac resistivity was determined by a four-point probe, in a closed-cycle helium cryostat, by applying a pulsed current of 0.1–1 mA. For temperatures lower than ≈20 K, samples were directly dipped into liquid helium. Magnetic susceptibility was measured by a Lake Shore Model 7000 ac susceptometer. Data were collected at a fixed frequency of 1 kHz and constant ac field amplitude ($h_{ac}=50\ \mu$T) on bar-shaped specimens. This allowed us to compare measurements performed on similar sized samples. Calibration was performed using a $Gd_2(SO_4)_3\cdot H_2O$ standard and demagnetization effects were taken into account.

Powder neutron diffraction data on selected samples were collected with the D2B diffractometer at Institute Max von Laue–Paul Langevin (Grenoble, France) in the high flux mode. Data were refined by the Rietveld method in the orthorhombic *Pmmm* space group using the GSAS refinement program. For all the Sr-substituted samples the thermal parameter of O4, the mobile oxygen, was unrealistically larger than those of other oxygen atoms in the structure. In the final refinement cycles O4 was placed at the $(x,\frac{1}{2},0)$ position, instead of $(0,\frac{1}{2},0)$, and x was allowed to vary. Reasonable values for x and the thermal parameters were obtained.

Electron microscopy analysis was carried out using a Philips CM microscope operating at 300 kV and equipped with a Kevex system for energy dispersive spectroscopy (EDS) analysis. The samples were crushed in a mortar with alcohol and the suspension was recovered onto an aluminum holey carbon grid. Electron diffraction patterns corresponding to different Ba-Sr ordering models were calculated by using the EMS software.[19]

III. RESULTS AND DISCUSSION

A. Phase characterization

Samples of $Y(Ba_{1-x}Sr_x)_2Cu_3O_w$ with $x\leqslant 0.5$ are single phase as shown by x-ray and neutron diffraction data. A

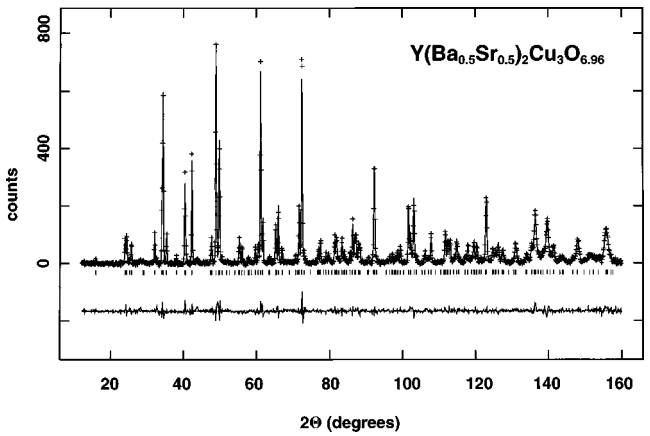

FIG. 1. Powder neutron diffraction pattern of $YBaSrCu_3O_{6.96}$ ($\lambda = 1.5943$ Å).

powder neutron diffraction pattern of the sample with $x = 0.5$ and $w = 6.96$ is shown as an example in Fig. 1. Samples with $x = 0.625$, 0.75, and 1 contain more than one phase and the content of impurities increases with x. As shown by x-ray diffraction, the sample corresponding to the nominal stoichiometry $YSr_2Cu_3O_w$ appears to contain mainly $SrCuO_2$, Y_2SrO_4, and possible traces of $Sr_{14-x}Y_xCu_{24}O_{41}$. The typical reflections of the phase 123 ($x = 1$), as reported in the literature,[9,10] are not present. The pattern of the sample with $x = 0.75$ contains the reflections of 123 together with those of Sr_2CuO_3. The reflections of Y_2SrO_4, observed in the pattern corresponding to $x = 1$, are not detectable and it is not clear whether the reflections of $SrCuO_2$ and $Sr_{14-x}Y_xCu_{24}O_{41}$ are present. The sample with $x = 0.625$ contains mainly the 123 phase. The reflections of secondary phases are weak and, except for that at $d \approx 2.87$ belonging to Sr_2CuO_3, they cannot be attributed with certainty to any known phase. In the impurity phases Ba and Sr form solid solutions as well, which makes it difficult to identify them by comparison with unsubstituted phases. For the $x = 0.625$ sample the sections in the diffraction pattern corresponding to the impurities were eliminated from the refinements. A list of the qualitatively identified phases in the powder patterns is reported in Table I as a function of x. The results are in reasonable agreement with those of Roth *et al.*[7]

B. Structural refinements as a function of x ($w > 6.9$)

The final results of the structural refinements are given in Tables II and III as a function of the Sr and O contents, respectively. The atoms are identified as shown in Fig. 2 and according to Ref. 20.

The oxygen stoichiometries determined by iodometric titration w_j are reported in the same tables. In general, they are in good agreement with those determined by structural refinements based on neutron diffraction data w_n, given by the sum of the occupation parameters of O4 and O5 sites, $w_n = 6 + n_{O4} + n_{O5}$, also shown in Tables II and III. The largest discrepancy between w_j and w_n, corresponding to 0.15 units in oxygen stoichiometry, is in the $x = 0.625$ sample; this could be attributed to the presence of impurities, which makes the iodometric titration results less reliable than those obtained by neutron diffraction.

All refined structures of $Y(Ba_{1-x}Sr_x)_2Cu_3O_w$ with $x \leqslant 0.625$ and $w \geqslant 6.685$ are orthorhombic (space group *Pmmm*). The strain, defined as $S = 2(b-a)/(b+a)$, is a nonlinear function of x. For $0 \leqslant x \leqslant 0.5$, the orthorhombic strain in $Y(Ba_{1-x}Sr_x)_2Cu_3O_w$ increases with x and is greater than in $YBa_2Cu_3O_w$. On the contrary, the strain for the phase with $x = 0.625$ is slightly smaller than that corresponding to the phase with $x = 0$, indicating that, as a function of x, the strain goes through a maximum. This is due to the different rates with which a and b vary with x. Figure 3 shows the variation of the lattice parameters a, b, and c and the strain S as a function of x. The b parameter decreases linearly with x. The parameter a decreases too, but not linearly. This decrease is mainly due to the shortening of the Ba/Sr-O4 bonds with x, which decrease more rapidly than the Cu1-O4 bond. The shortening of the latter is responsible for the decrease of b. For small values of x the decrease of a is steeper than that of b and this results in the increase of the strain. For a further increase of x, however, the occupancy factor of the O5 site, situated as O4 in the basal plane, increases (see Table II). This occupation attenuates the decrease of a since the surroundings of the Sr cations with respect to the basal plane becomes less anisotropic. The attenuation results in the decrease of the strain and a maximum is observed between $x = 0.25$ and 0.5 (see Fig. 3). The strain calculated with the present data is somewhat different from that reported by Veal *et al.* for a sample with $x = 0.5$.[5] From the results of the $x = 0.5$ sample as a function of w (see Table III) it can be deduced that the data of Veal *et al.* might correspond to a phase with an oxygen content lower than 6.9.

The nonlinearity of the S vs x curve does not allow us to evaluate the Sr concentration at which the phase becomes tetragonal for $w \geqslant 6.9$. The $YSr_2Cu_3O_w$ phase ($w \approx 7$) reported by Okai[9] is tetragonal as $YSr_2Re_yCu_{3-y}O_w$ with a small Re content ($y \approx 0.15$).[10,21]

No variation as a function of x was found for the buckling of the Cu2 squares. The Cu2-O2-Cu2 and Cu2-O3-Cu2 angles remain constant within one or two standard deviations at about 163.0° and 164.5°, respectively.

Table IV shows the variations of some structural parameters ($\Delta\mathcal{P}$) for a given Sr content interval Δx normalized to the same parameter value at $x = 0$, $\mathcal{P}_{x=0}$

TABLE I. Qualitative x-ray phase analysis in $Y(Ba_{1-x}Sr_x)_2Cu_3O_w$, as a function of x.

	Phases						
nominal x	123	$(Sr,Y)_{14}Cu_{24}O_{41}$	Sr_2CuO_3	$SrCuO_2$	Y_2SrO_4	$Y_2Cu_2O_5$	Y_2O_3
0.625	≈90%	possible	trace	no	no	no	no
0.75	⩽50%	possible	present	possible	possible	possible	possible
1	no	present	possible	present	present	possible	possible

TABLE II. Structural parameters of $Y(Ba_{1-x}Sr_x)_2Cu_3O_w$ as a function of x for $w \geqslant 6.90$. Rietveld refinements were done in the orthorhombic *Pmmm* space group. Atom positions are $Y(\frac{1}{2},\frac{1}{2},\frac{1}{2})$, $Ba/Sr(\frac{1}{2},\frac{1}{2},z)$, $Cu1(0,0,0)$, $Cu2(0,0,z)$, $O1(0,0,z)$, $O2(\frac{1}{2},0,z)$, $O3(0,\frac{1}{2},z)$, $O4(x,\frac{1}{2},0)$, and $O5(\frac{1}{2},0,0)$. Numbers in parentheses are statistical standard deviations of the last significant digit.

Compound		$x=0$[a]	$x=0.25$	$x=0.5$	$x=0.625$
Y	$B(A)$	0.28(3)	0.31(6)	0.34(6)	0.51(10)
Ba/Sr	z	0.1843(2)	0.184 53(23)	0.184 43(24)	0.1863(4)
	$B(A)$	0.44(3)	0.55(6)	0.84(7)	0.80(11)
Cu1	$B(A)$	0.41(3)	0.41(6)	0.68(7)	0.35(11)
Cu2	z	0.3556(1)	0.353 64(16)	0.352 09(17)	0.352 33(27)
	$B(A)$	0.20(2)	0.33(5)	0.39(5)	0.29(8)
O1	z	0.1590(2)	0.158 89(23)	0.159 52(27)	0.1580(5)
	$U11$	0.009(1)	0.0320(3)	0.0408(4)	0.0134(9)
	$U22$	0.007(1)	0.0119(2)	0.0225(3)	0.0040(6)
	$U33$	0.010(1)	0.0013(1)	0.0008(2)	0.0094(5)
	n	2.06(2)			
O2	z	0.3779(2)	0.377 78(22)	0.376 70(24)	0.3742(4)
	$B(A)$	0.51(4)	0.47(6)	0.47(7)	0.43(11)
O3	z	0.3790(2)	0.376 37(24)	0.374 58(26)	0.3756(4)
	$B(A)$	0.35(3)	0.30(6)	0.37(7)	0.28(11)
O4	x		0.0399(13)	0.0572(30)	0.052(7)
	$U11$	0.022(3)	0.0259(5)	0.0365(8)	0.1954(37)
	$U22$	−0.001(2)	0.0259(5)	0.0365(8)	0.1954(37)
	$U33$	0.019(2)	0.0259(5)	0.0365(8)	0.1954(37)
	n	0.9	0.934(9)	0.868(10)	0.972(18)
O5	n	0.03(1)	0.044(9)	0.085(10)	0.098(16)
a (Å)		3.8227(1)	3.799 76(8)	3.785 26(9)	3.783 97(17)
b (Å)		3.8872(2)	3.870 28(10)	3.853 13(11)	3.845 16(21)
c (Å)		11.6802(2)	11.621 45(29)	11.562 00(30)	11.539 96(53)
V (Å^3)		173.56	170.9064(71)	168.6328(77)	167.9062(143)
Cu2-O2 (Å)		1.9290	1.9205(4)	1.9139(5)	1.9088(7)
Cu2-O3 (Å)		1.9627	1.9531(4)	1.9440(5)	1.9413(8)
Cu2-O1 (Å)		2.29632	2.2633(30)	2.2265(34)	2.243(6)
Cu1-O1 (Å)		1.8571	1.8465(27)	1.8444(31)	1.823(6)
Ba/Sr-O1 (Å)		2.7418	2.7282(4)	2.7160(5)	2.7171(9)
Cu2-Cu2 (Å)		3.3732	3.401 83(32)	3.420 27(34)	3.4082(54)
R_{wp} (%)/R_{expt} (%)		5.96/3.33	6.63/5.1	6.85/5.27	7.55/6.03
$(b-a)/(b+a)\times 10^3$		8.366	9.194	8.886	8.021
w_j (iodometric)		6.93	6.95	6.96	6.92
w_n (neutron)			6.98	6.95	7.07

[a]Data from Jorgensen *et al.* (Ref. 24).

$[\Delta\mathcal{P}/\Delta x)/\mathcal{P}_0(x^{-1})]$. If compared with the values of Jorgensen *et al.*,[2] which correspond to the variations induced by external pressure in the $YBa_2Cu_3O_{6.93}$ structure $[\Delta\mathcal{P}/\Delta P)/\mathcal{P}_{P=\text{amb}}(P^{-1})]$, the values of Table IV indicate the following.

(i) the complete substitution of Ba with Sr ($x=1$) would induce a variation (extrapolated value) of the lattice parameters equivalent to the application of an external pressure of about 10 GPa.

(ii) the contraction of the three parameters resulting from the application of the chemical pressure is almost isotropic along the three directions, whereas that induced by external pressure is highly anisotropic. The pressure-induced contraction along the c axis is twice as much as that observed along the other two axis.

(iii) The Cu2-O1 distance, that is, the distance from the Cu of the pyramids and the apical oxygen O1, decreases with increasing Sr. This reduction is three times greater than that of the c axis ($[\Delta(\text{Cu2-O1})/\Delta x]/(\text{Cu2-O1})_{x=0} = -60\times 10^{-3}$ against $(\Delta c/\Delta x)/c_{x=0} = -20\times 10^{-3}$). The Cu1-O1 distance decreases slightly and the coefficient ($[\Delta(\text{Cu1-O1})/\Delta x]/(\text{Cu1-O1})_{x=0}$) is smaller than that corresponding to the c axis (-13.7×10^{-3} against -20.2×10^{-3}). As a function of external pressure, the Cu2-O1 distance decreases as the c axis does, whereas the Cu1-O1 distance also decreases, but at a lower rate. For $P\approx 0.6$ GPa the decrease can be evaluated at about 0.5% of the value at $P=1$ atm.[2] With increasing x, O1 tends to move towards a symmetrical position between Cu1 and Cu2 and T_c decreases. This seems to contradict the speculation made by Brown[22] according to

TABLE III. Structural parameters of $Y(Ba_{1-x}Sr_x)_2Cu_3O_w$ as a function of w for $x=0.5$. Rietveld refinements were done in the orthorhombic *Pmmm* space group. Atom positions are $Y(\frac{1}{2},\frac{1}{2},\frac{1}{2})$, $Ba/Sr(\frac{1}{2},\frac{1}{2},z)$, Cu1(0,0,0), Cu2(0,0,$z$), O1(0,0,$z$), O2($\frac{1}{2}$,0,$z$), O3(0,$\frac{1}{2}$,$z$), O4($x$,$\frac{1}{2}$,0), and O5($\frac{1}{2}$,0,0). Numbers in parentheses are statistical standard deviations of the last significant digit.

		Oxygen content w_j-w_n			
Compound		6.98−6.97	6.96−6.95	6.80−6.82	6.685−6.74
Y	$B(A)$	0.39(5)	0.34(6)	0.50(7)	0.31(5)
Ba/Sr	z	0.184 80(20)	0.184 43(24)	0.188 41(25)	0.189 67(20)
	$B(A)$	0.73(6)	0.84(7)	0.84(7)	1.08(6)
Cu1	$B(A)$	0.63(6)	0.68(7)	0.78(8)	0.86(7)
Cu2	z	0.351 92(14)	0.352 09(17)	0.353 55(18)	0.354 56(14)
	$B(A)$	0.29(4)	0.39(5)	0.26(5)	0.40(4)
O1	z	0.158 87(22)	0.159 52(27)	0.156 54(31)	0.157 73(25)
	$U11$	0.0515(3)	0.0408(4)	0.1369(8)	0.1225(5)
	$U22$	0.0174(2)	0.0225(3)	0.0458(4)	0.1076(4)
	$U33$	0.0007(1)	0.0008(2)	0.0004(1)	0.0049(1)
O2	z	0.376 20(20)	0.376 70(24)	0.375 84(27)	0.376 44(31)
	$B(A)$	0.45(5)	0.47(7)	0.43(7)	0.52(6)
O3	z	0.374 80(21)	0.374 58(26)	0.375 45(29)	0.375 03(31)
	$B(A)$	0.32(5)	0.37(7)	0.48(7)	0.55(6)
O4	x	0.0536(26)	0.0572(30)	0.059(5)	0.073(4)
	$U11$		0.0142(8)		0.1136(22)
	$U22$		0.0142(8)		0.1136(22)
	$U33$		0.0142(8)		0.1136(22)
	n	0.900(8)	0.868(10)	0.688(12)	0.598(13)
O5	n	0.068(8)	0.085(10)	0.133(12)	0.143(12)
a (Å)		3.784 09(8)	3.785 26(9)	3.801 74(12)	3.817 28(11)
b (Å)		3.853 74(9)	3.853 13(11)	3.850 09(14)	3.841 03(11)
c (Å)		11.562 79(24)	11.562 00(30)	11.5739(4)	11.584 58(33)
V (Å^3)		168.6191(62)	168.6328(77)	169.4073(100)	169.8566(84)
Cu2-O2 (Å)		1.9128(4)	1.991 39(5)	1.9183(5)	1.9254(5)
Cu2-O3 (Å)		1.9450(4)	1.9440(5)	1.9417(5)	1.9351(5)
Cu2-O1 (Å)		2.2322(28)	2.2265(34)	2.280(4)	2.2801(33)
Cu1-O1 (Å)		1.8370(26)	1.8444(31)	1.812(4)	1.8273(29)
Ba/Sr-O1 (Å)		2.7171(4)	2.7160(5)	2.7304(7)	2.7328(5)
Cu2-Cu2 (Å)		3.424 43(28)	3.420 27(34)	3.390 00(36)	3.3697(28)
R_{wp} (%)/R_{expt} (%)			6.85/5.27		6.59/5.11
$(b-a)/(b+a)\times 10^3$		9.119	8.888	6.319	3.101

which a symmetrical position of O1 with respect to Cu1 and Cu2 would favor charge delocalization with the consequent increase of T_c.

(iv) The thickness of the $(Cu2O_2)(Y)(Cu2O_2)$ superconducting block, measured by the Cu2-Cu2 distance, increases with increasing x, while it decreases with increasing pressure (Fig. 4). This is the only parameter that behaves oppositely with increasing x or with increasing P. A similar situation was observed for the corresponding block in Hg-1223 when either this compound is subjected to an external pressure or the Ba cations are substituted by Sr.[14] In the latter structure the superconducting block comprises five layers, CuO2-Ca-CuO2-Ca-CuO2, and the thickness is defined as the distance between the Cu cations of the external layers.

(v) In $Y(Ba_{1-x}Sr_x)_2Cu_3O_w$ the chemical pressure induces a displacement δ of O4 from the b axis. O4 moves from the $(0,\frac{1}{2},0)$ to the $(x,\frac{1}{2},0)$ position. The values of $\delta=xa$ (x is the

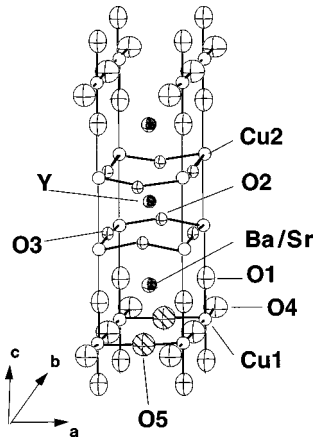

FIG. 2. Schematic structure of $Y(Ba_{1-x}Sr_x)_2Cu_3O_w$ showing the labeling of atoms. The shading of O5 indicates partial occupation.

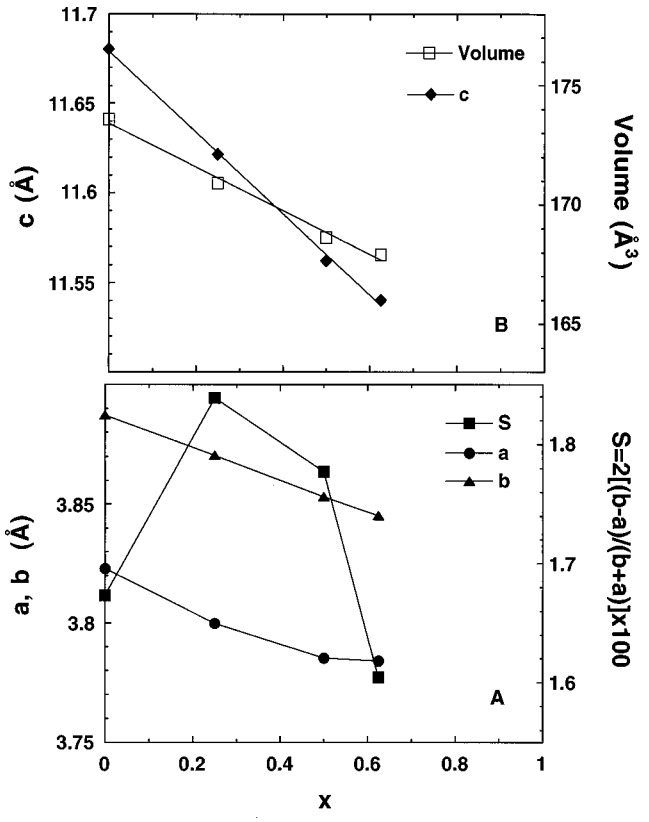

FIG. 3. Cell parameters and orthorhombic strain $S=[2(b-a)/(b+a)]\times 10^2$ of $Y(Ba_{1-x}Sr_x)_2Cu_3O_{>6.9}$ as a function of x. Error bars are smaller than the size of the symbols. The lines are guides for the eyes.

coordinate along the a axis) are shown in Fig. 5 as a function of the Sr concentration. This displacement, which does not occur when an external pressure is applied, is mainly due to the difference in size of Sr and Ba and increases from $x=0$ to 0.5. We found a maximum in the δ vs x plot since the value of δ for $x=0.625$ is smaller than that for $x=0.5$, but the two values differ by only one standard deviation. It can be argued that for $x=1$, when all Ba/Sr sites are occupied by the same cation, the displacement goes to 0. However, from our experimental data we cannot rule out that the O4 displacement is intrinsic to the structure of 123 compounds. For example, François *et al.*[23] found that in the structure of $YBa_2Cu_3O_w$ with $w=6.91$ and 6.86, O4 is displaced from

TABLE IV. Linear and volume compressibility of structural parameters in $Y(Ba_{1-x}Sr_x)_2Cu_3O_w$ as a function of x.

$(\Delta a/\Delta x)/a_0(x^{-1})$	-19.6×10^{-3}
$(\Delta b/\Delta x)/b_0(x^{-1})$	-17.5×10^{-3}
$(\Delta c/\Delta x)/c_0(x^{-1})$	-20.2×10^{-3}
$(\Delta V/\Delta x)/V_0(x^{-1})$	-56.8×10^{-3}
$[\Delta(\text{Cu2-O1})/\Delta x]/(\text{Cu2-O1})_0(x^{-1})$	-60.8×10^{-3}
$[\Delta(\text{Cu1-O1})/\Delta x]/(\text{Cu1-O1})_0(x^{-1})$	-13.7×10^{-3}
$[\Delta(\text{Cu2-Cu2})/\Delta x]/(\text{Cu2-Cu2})_0(x^{-1})$	$+27.9\times10^{-3}$
$[\Delta(\text{Ba/Sr-Ba/Sr})/\Delta x]/(\text{Ba/Sr-Ba/Sr})_0(x^{-1})$[a]	-22.2×10^{-3}

[a]The z in this case was assumed as the arithmetic average of $z(\text{Ba/Sr})$ and $z(\text{O1})$ (Table II).

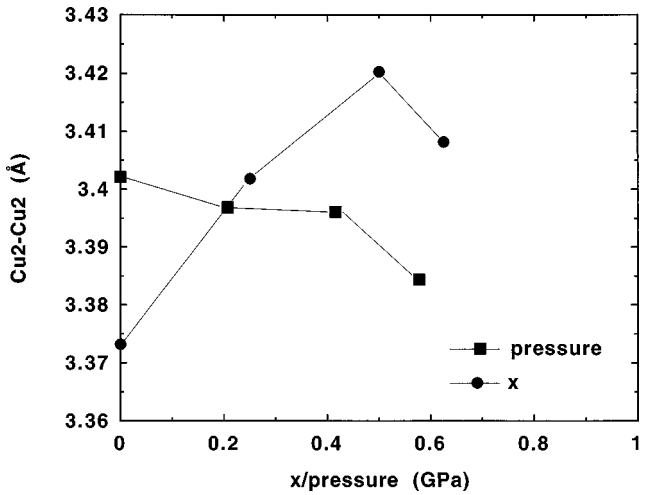

FIG. 4. Superconducting CuO_2-Y-CuO_2 block thickness in $Y(Ba_{1-x}Sr_x)_2Cu_3O_{>6.9}$ as a function of x and of P. The numbers on the abscissa represent either x (from 0 to 1 in the chemical formula) or pressure (from 0 to 1 GPa). Error bars are smaller than the size of the symbols. The lines are guides for the eyes.

the $(0,\frac{1}{2},0)$ to the $(x,\frac{1}{2},0)$ position. Their data indicate that δ slightly increases with decreasing w.

C. Structural refinement as a function of w ($x=0.5$)

The final structural parameter values obtained after the structural refinements of the samples with $x=0.5$ and varying oxygen stoichiometry are reported in Table III. The linear and volume compressibilities of several parameters as a function of w are shown in Table V and Fig. 6. If these parameters are compared with those of the phases with $x=0$ as a function of w,[24] a great similarity is observed. In particular, a, c, and V increase with decreasing w, while b decreases. For the phases with $x=0.5$, a decrease of w leads to a reduction of the strain. $S=0$, namely, the tetragonal symmetry, is obtained at about $w=6.6$ (see Fig. 6). This value is sensibly higher than that obtained for $YBa_2Cu_3O_w$, for which $S=0$ is obtained at $w\approx6.35$. The occupation of the O5 site, which is responsible for the orthorhombic to

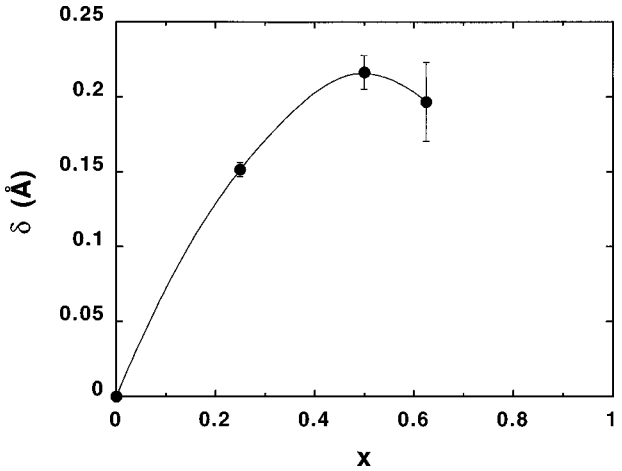

FIG. 5. Displacement of O4 from the $(0,\frac{1}{2},0)$ position δ in $Y(Ba_{1-x}Sr_x)_2Cu_3O_{>6.9}$ as a function of x. The line is a guide for the eyes.

TABLE V. Linear and volume compressibility of structural parameters in $YBaSrCu_3O_w$ as a function of oxygen stoichiometry. $w^*=6.96$, corresponding to the oxygen stoichiometry at which $T_c = T_{c\,\max}$.

$(\Delta a/\Delta w)/a_{w^*}(w^{-1})$	3.08×10^{-2}
$(\Delta b/\Delta w)/b_{w^*}(w^{-1})$	-1.14×10^{-2}
$(\Delta c/\Delta w)/c_{w^*}(w^{-1})$	0.71×10^{-2}
$(\Delta V/\Delta w)/V_{w^*}(w^{-1})$	2.64×10^{-2}
$[\Delta(\text{Cu2-O1})/\Delta w]/(\text{Cu2-O1})_{w^*}(w^{-1})$	8.75×10^{-2}
$[\Delta(\text{Cu1-O1})/\Delta w]/(\text{Cu1-O1})_{w^*}(w^{-1})$	-3.37×10^{-2}
$[\Delta(\text{Cu2-Cu2})/\Delta w]/(\text{Cu2-Cu2})_{w^*}(w^{-1})$	-5.38×10^{-2}

tetragonal transition in the 123 structure, is $n_{O5}=0.068(8)$ at $w\approx6.98$. A similar occupation factor for O5 in 123 with $x=0$ is obtained at $w\approx6.45$.[24]

The decrease of the oxygen content causes a shortening of the Ba/Sr-O4 distance, which results in an increase of the displacement δ of O4 from the $(0,\frac{1}{2},0)$ position (Table III). This strongly indicates that the oxygen that is removed from the structure is the one surrounding Ba. Since the large sites are occupied simultaneously by Ba and Sr, the Ba/Sr-O distance corresponds to the average of the two distances Ba-O and Sr-O, with the former being larger than the latter. The precise refinements of the YBCO structure as a function of oxygen stoichiometry carried out by Jorgensen *et al.*[24] and Cava *et al.*[20] did not investigate the possible displacement of O4. As stated above, François *et al.*[23] did study this feature and found a displacement of O4 from the $(0,\frac{1}{2},0)$ position. Specific experiments are necessary for establishing a definite relationship between δ and w.

D. Electron microscopy

In an attempt to verify the occurrence of some ordering in the Ba and Sr distribution, samples with nominal composition $YBaSrCu_3O_{6.96}$ were examined by electron microscopy. EDS results confirmed a 1:1:1 ratio for Ba:Sr:Y. Electron diffraction patterns were obtained along several zone axes. Along [001] (Fig. 7), the pattern is similar to that obtained for the unsubstituted Ba compound and the splitting of the reflections indicates that the crystallites are twinned with the presence of two variants. As for $YBa_2Cu_3O_{6.9}$ (001) is the twinning plane. However, as soon as one tilts the crystallites around the $\langle100\rangle^*$ or $\langle110\rangle^*$ axis, diffuse scattering appears around the Bragg reflections in the form of crosses whose branches are oriented along a^* (or b^*) (Fig. 8). The intensity of the diffuse scattering is enhanced at the extremities of the crosses, giving rise to satellites. From the observation of successive zone axis patterns obtained by tilting around the $\langle100\rangle^*$ or $\langle110\rangle^*$, it has been possible to localize the diffuse scattering in the reciprocal space. The crosses are centered at positions $(hkl/2)$ and their branches are about $a^*/4$ long. We assumed that this additional diffuse scattering is due to a Ba/Sr ordering. It is well defined along c and the presence of reflections with $l/2$ suggests the doubling of the c axis. In the ab plane there is probably an ordering of Ba and Sr, which gives rise to a $4a$ periodicity, but the ordering should be short ranged.

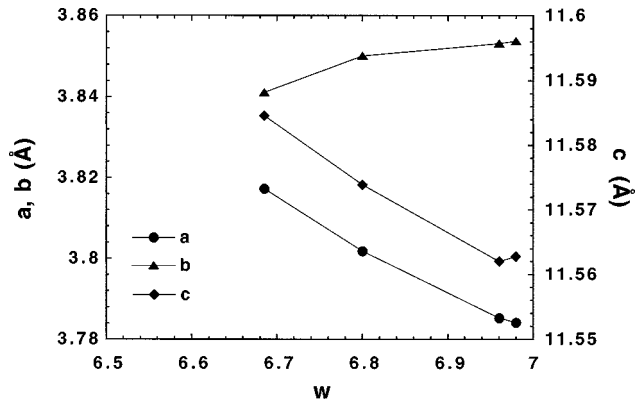

FIG. 6. Cell parameters of $YBaSrCu_3O_w$ as a function of w. Error bars are smaller than the size of the symbols. The lines are guides for the eyes.

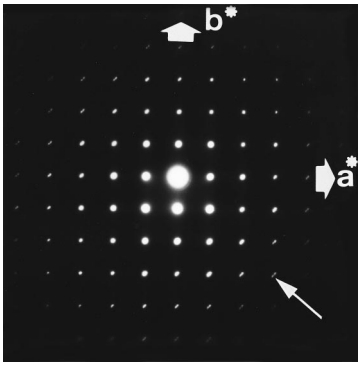

FIG. 7. Electron diffraction pattern taken along the [001] zone axis. The splitted reflections due to twinning are indicated by an arrow.

E. Superconductivity

The values of T_c as a function of x and w (at fixed x), determined from ac resistivity measurements versus T, are reported in Figs. 9 and 10. The diamagnetic shielding $\mathcal{S}$, expressed as the percent of $4\pi\rho\chi'$ [where ρ is the density (g/cm^3) and χ' is the specific susceptibility (cm^3/g)], and the diamagnetic onset of T_c are reported in Table VI. The resistivity data show a linear decrease of T_c with x at a rate of $20\ \text{K}/x$. The bars in Fig. 9 represent the transition width, defined as the 90–10 % interval of the transition. It is worthwhile mentioning that the transition of the compound with

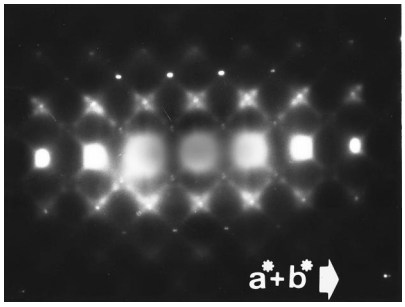

FIG. 8. Electron diffraction pattern obtained after a slight tilt around the $[1\bar{1}0]$ axis from the [001] zone axis. Crosses consisting of diffuse scattering are seen with satellites at about $a^*/4$ from the center.

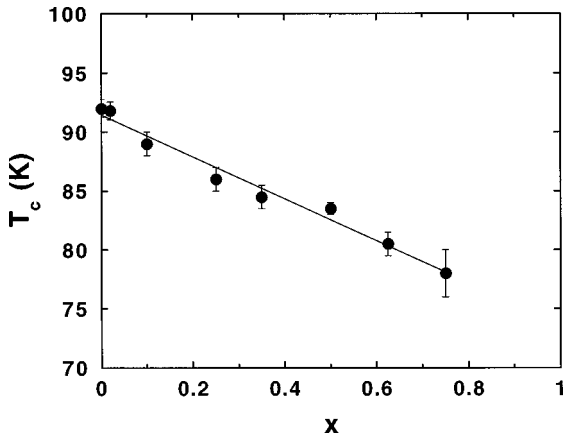

FIG. 9. Resistive T_c of $Y(Ba_{1-x}Sr_x)_2Cu_3O_{>6.96}$ as a function of x. $T_c = T$ at the midpoint of the transition. Bars represent the temperature interval for the complete transition.

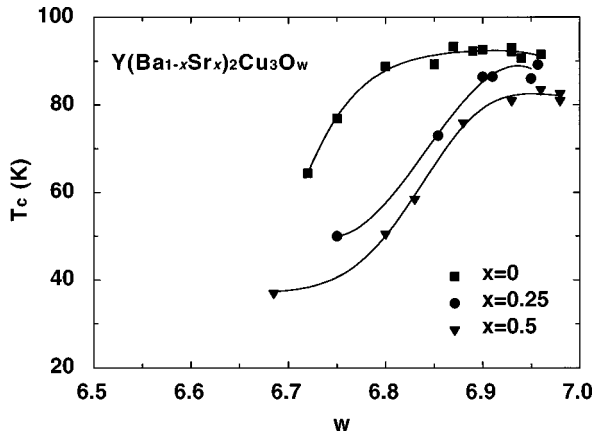

FIG. 10. Resistive transition of $Y(Ba_{1-x}Sr_x)_2Cu_3O_w$ as a function of w at fixed x. The lines are guides for the eyes.

$x = 0.5$ is the narrowest one and the corresponding T_c is higher than the value extrapolated from the T_c vs x plot. This corroborates the ordering between Ba and Sr found by electron diffraction.

The value of T_c for the polyphasic sample with $x = 0.75$ falls exactly on the T_c vs x curve. This indicates that the solubility of Sr in $Y(Ba_{1-x}Sr_x)_2Cu_3O_w$ does not saturate at $x \approx 0.625$, in agreement with the results of Veal *et al.*,[5] and thus could mean that T_c depends upon parameters other than x. The T_c onset determined from susceptibility measurements remains almost unchanged at $T \approx 81$ K in compounds with $x \geqslant 0.625$. This is probably due to the polyphasic nature of the samples containing traces of the 123 phases with $x \leqslant 0.75$ that are responsible for the higher diamagnetic drops. Such a hypothesis is corroborated by the fact that the transition is broad (more than 10 K) and the diamagnetic fraction is small ($\mathcal{S} \lesssim 20\%$ at 5 K). The polyphasic sample with $x = 1$ does not exhibit any transition either resistive or diamagnetic down to 4.2 K. By extrapolating to $x = 1$, the T_c vs x plot gives a value of ≈ 70 K, which is larger than that measured by Okai ($T_c \approx 60$ K) in the material synthesized at 7 GPa.[9] As pointed out by the same author, this would suggest that the $YSr_2Cu_3O_w$ compound might be somewhat different from the homolog $YBa_2Cu_3O_w$.

Like the $x = 0$ compound, the T_c of each Sr-substituted material increases with increasing w. The w^* doping, taken as that corresponding to the highest T_c for a fixed x, seems to increase with x, as shown in Fig. 10 and summarized in Table VII.

TABLE VI. Resistive and diamagnetic T_c of $Y(Ba_{1-x}Sr_x)_2Cu_3O_w$, as a function of x and w. Letters in column 3 correspond to annealing treatments, as explained in the text. *m* denotes a multiphase compound and ns denotes not superconducting down to 4.2 K.

x	w_j	Annealing	Resistive T_c (K)[a]	Diamagnetic onset	Percent of diamagnetic shielding (at 5 K)
0	6.94	*A*	90.5	92.5	100
0	6.87	*G*	93.5	93.5	100
0	6.90	*R*	92.6	92.4	100
0.25	6.96	*A*	89	87.2	98[b]
0.5	6.98	*A*	82	83	100
0.5	6.96	*A*	83.5	83.5	100
0.5	6.80	*R*	51.5	45.5	62
0.5	6.685	*G*	34	34.2	51
0.625	6.91	*A*	80	81	84
0.625	6.94	*A*	74	81.2	81.5[b]
0.75	m	*A*	80	81	21
0.75	m	*R*	75	81	18
0.75	m	*S*	78	81	16
1.00	m	*A*	ns	ns	
1.00	m	*R*	ns	ns	
1.00	m	*S*	ns	ns	

[a] T at the midpoint of the transition.
[b] Values at 77 K.

F. Bond valence sum, stress, and hole density

In order to see if the decreases in T_c induced by the Sr substitution could be understood in terms of a reduction of charge transfer, the bond valence sums[25] (BVS's) for the different cations, as a function of x and w, were calculated. In Table VIII we report the average Cu valences, calculated from either w_j and w_n and by assuming for Y, Ba/Sr, and O the fixed valences of 3+, 2+, and 2−, respectively. In the same table we report the BVS values for Cu1, Cu2, Ba/Sr and Y, calculated by the formula

$$V_i = \sum s_{ij} = \sum \exp[(R_0 - R_{ij})/B], \qquad (1)$$

TABLE VII. $T_{c\,\max}$ as a function of x. $T_c^* = T_c$ at $w = 6.87$ and $w^* = w$ at which $T_{c\,\max}$ was obtained.

x	$T_c^*/T_{c\,\max}$	w^*
0	1	6.87
0.25	0.89	6.96
0.5	0.85	6.96
0.625	0.91	6.91

TABLE VIII. Experimental and calculated valence V of Cu1, Cu2, Ba/Sr, and Y as a function of x and w. V_j was determined by iodometric titration, V_n was determined by neutron data, and V_{BVS} was calculated from Eq. (1). The constants used for calculations were taken from Ref. 26 and correspond to the following. $B=0.37$. $R_o(Cu^{2+}/Cu^{3+})$ is equal to the weighted average of $R_o(Cu^{2+})=1.679$ and $R_o(Cu^{3+})=1.73$. The Cu^{2+}/Cu^{3+} ratio was calculated on the basis of the measured $(V_j+V_n)/2$ values. $R_o(Ba^{2+}/Sr^{2+})$ is equal to the weighted average of $R_o(Ba^{2+})=2.285$ and $R_o(Sr^{2+})=2.118$. $R_o(Y^{3+})=2.019$.

	Cu1			Cu2			Ba/Sr	Y
x-w_j-w_n	V_i	V_n	V_{BVS}	V_i	V_n	V_{BVS}	V_{BVS}	V_{BVS}
0-6.93[a]	2.29	2.29	2.30	2.29	2.29	2.19	2.17	2.88
0-6.95[b]	2.30	2.30	2.38	2.30	2.30	2.21	2.19	2.905
0.25-6.95-6.98	2.30	2.32	2.34	2.30	2.32	2.30	2.14	2.93
0.5-6.96-6.95	2.31	2.30	2.33	2.31	2.30	2.36	2.03	2.93
0.625-6.92-7.07	2.28	2.38	2.56	2.28	2.38	2.38	1.98	2.92
0.5-6.98-6.97	2.32	2.31	2.38	2.32	2.31	2.36	2.03	2.93
0.5-6.80-6.82	2.20	2.21	2.29	2.20	2.21	2.29	1.93	2.90
0.5-6.685-6.74	2.12	2.16	2.12	2.12	2.16	2.27	1.91	2.89

[a]RT data of Brown (Ref. 25).
[b]5 K data of Cava *et al.* (Ref. 20).

where V_i represents the valence of the ion i, R_0 is a specific parameter of the ion i for a given valence, R_{ij} is the experimental distance between the ion i and the first nearest neighbors j, and B is a universal constant equal to 0.37.[25] The R_0 values were taken from Ref. 26 and are indicated in Table VIII. For the Ba/Sr site, R_0 was assumed as the weighted arithmetic average of $R_0(Sr^{2+})$ and $R_0(Ba^{2+})$. For Cu, a weighted average of $R_0(Cu^{2+})$ and $R_0(Cu^{3+})$ was calculated from the measured w value. Based on this hypothesis, the valence of Cu1 is almost x independent from $x=0$ to 0.5, while it increases abruptly between $x=0.5$ and 0.625 from 2.33 to 2.57. On the other hand, for x increasing from 0 to 0.625 the valence of Cu2 increases monotonically from $\approx$2.20 to 2.36. The BVS of the Ba/Sr site decreases with increasing x and reaches values very close to the formal valence of these cations at $x \geqslant 0.5$ (2.03 and 1.98 at $x=0.5$ and 0.625, respectively). For x increasing from 0.25 to 0.625 the BVS for Y remains almost unchanged at $\approx$2.93. This indicates that the Sr substitution almost completely reduces the stress on the large cation layers.[22]

The increase of T_c with increasing w in $YBa_2Cu_3O_w$ is due to the charge transfer from the chain to the plane copper. The transfer is enabled by the stress of the Ba-O layers. According to the values quoted by Cava *et al.*,[20] the BVS for Ba in $YBa_2Cu_3O_{6.96}$ is 2.18 valence units. This means that the stress corresponds to 0.18. Thus the Ba-O interatomic distances are smaller than the value corresponding to a formal valence of 2+. Consequently, the Cu2-O distances are smaller than the value corresponding to Cu^{2+}-O distance and the Cu2 cations can accept the extra charges of Cu1 coming from the extra oxygen.

Here we suggest that the stress of the Ba layer plays an important role in the charge transfer from Cu1 to Cu2. The relaxation of this layer due to the Sr substitution does not allow the substituted compounds to reach the doping level of the unsubstituted one. This model is based on the assumption that the hole density on the CuO_2 layer is the key factor determining T_c.

In Fig. 11 the differences between the formal valence and the calculated BVS for the Ba/Sr and Cu sites are reported. The formal valence of Ba/Sr is taken as 2+, while that of Cu is the valence measured by iodometric titration. The variation of these differences, which is a measure of the stress, for increasing x is the same as that observed for decreasing w for $x=0$.[22] It is worthwhile mentioning that in both cases T_c decreases.

As can be seen from Fig. 12, the average BVS for Cu1 and Cu2 increases with increasing Sr content. This is not in agreement with the data reported in Table VIII, where the average Cu valence, measured by either iodometric titration or neutron diffraction, remains constant. This discrepancy is probably due to a remnant stress in one or both CuO layers. By varying the oxygen stoichiometry from 6.98 to 6.685 in $YBaSrCu_3O_w$, the BVS's of Ba, Y, Cu1, and Cu2 decrease with decreasing w, which is in agreement with what has been observed in the unsubstituted compound.[20]

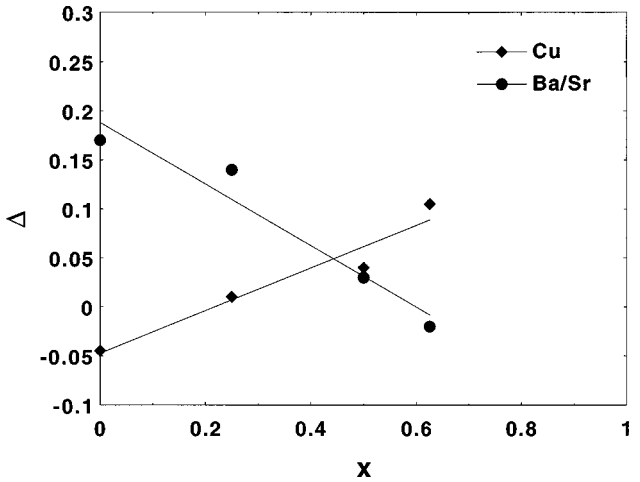

FIG. 11. Difference between calculated BVS and formal or measured values for the Ba/Sr and Cu^{2+}/Cu^{3+} sites, respectively. The lines are guides for the eyes.

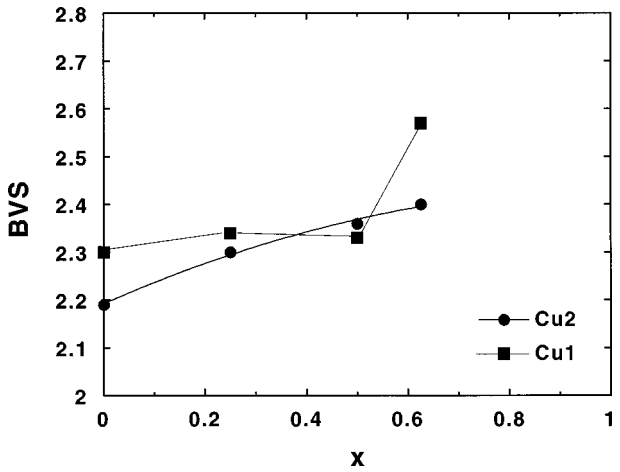

FIG. 12. BVS's of Cu1 and Cu2 as functions of x. The lines are guides for the eyes.

IV. CONCLUSIONS

In order to unveil the structural mechanism responsible for the decrease of T_c when Ba cations are replaced by Sr in $YBa_2Cu_3O_w$, several solid solutions of the system $Y(Ba_{1-x}Sr_x)_2Cu_3O_w$ were synthesized and characterized. Monophasic samples were obtained up to $x=0.5$. At $x=0.75$ the amount of impurities is more than 50%, while the ''123'' phase does not form for $x=1$. As x increases, T_c decreases monotonically from 92.5 K for $x=0$ to 78 K for $x=0.75$. As shown by powder neutron diffraction most of the structural parameters decrease with x just as they decrease when the unsubstituted compound is subjected to mechanical pressure. However, in the latter case an increase of T_c is observed. The only structural parameter that exhibits opposite behavior with respect to the application of the two types of pressures, mechanical and chemical, is the thickness of the superconducting block, which is the distance between two Cu of the same $(CuO_2)(Y)(CuO_2)$ block. The T_c dependence on w for $x=0.5$ reveals that the same parameter increases for increasing w, which corresponds to an increase of T_c. This suggests that the thickness of the superconducting block is not the parameter controlling T_c in this system. Short-range order has been detected by electron diffraction for the compound with $x=0.5$. This compound exhibits the sharpest transition, even sharper than that of the unsubstituted compound. The BVS's calculated as a function of x reveal that the Sr substitution releases the stress of the Ba/SrO layers and this relaxation hinders the charge transfer at a given oxygen concentration. It is suggested that this reduction of charge transfer is the key factor for the decrease of T_c. For the system $Y(Ba_{1-x}Sr_x)_2Cu_3O_w$ the value of w corresponding to the maximum T_c increases with x, thus the Sr substitution enlarges the underdoped region.

ACKNOWLEDGMENTS

We would like to thank T. Besagni and P. Ferro for their technical assistance during the sample preparation and chemical analysis.

*Author to whom correspondence should be addressed. Electronic address: licci@maspec.bo.cnr.it

[1] See, for example R. Benischke, T. Weber, W. H. Fietz, J. Metzger, K. Grube, T. Wolf, and H. Wuhl, Physica C **203**, 293 (1992), and references therein.
[2] J. D. Jorgensen, S. Pei, P. Lightfoot, D. G. Hinks, B. W. Veal, B. Dabrowski, A. P. Paulikas, R. Kleb, and I. D. Brown, Physica C **171**, 93 (1990).
[3] J. Metzger, T. Weber, W. H. Fietz, K. Grube, H. A. Ludwig, T. Wolf, and H. Wuhl, Physica C **214**, 371 (1993).
[4] T. Wada, S. Adachi, T. Mihara, and R. Inaba, Jpn. J. Appl. Phys., Part 2 **26**, L706 (1987).
[5] B. W. Veal, W. K. Kwok, A. Umezawa, G. W. Crabtree, J. D. Jorgensen, J. W. Downey, L. J. Nowicki, A. W. Mitchell, A. P. Paulikas, and C. H. Sowers, Appl. Phys. Lett. **51**, 279 (1987).
[6] A. Ono, T. Tanaka, H. Nozaki, and Y. Ishizawa, Jpn. J. Appl. Phys., Part 2 **26**, L1687 (1987).
[7] R. S. Roth, C. J. Rawn, J. D. Whitler, C. K. Chiang, and W. K. Wong-ng, J. Am. Ceram. Soc. **72**, 395 (1989).
[8] M. Oda, T. Murakami, Y. Enomoto, and M. Suzuki, Jpn. J. Appl. Phys., Part 2 **26**, L804 (1987).
[9] B. Okai, Jpn. J. Appl. Phys., Part 2 **29**, L2180 (1990).
[10] T. Den and T. Kobayashi, Physica C **196**, 141 (1992).
[11] D. E. Morris, K. K. Singh, V. Kirtikar, and A. P. B. Sinha, Physica C **235-240**, 903 (1994).
[12] M. A. Subramanian and M.-H. Whangbo, J. Solid State Chem. **109**, 410 (1994).
[13] S. Hahakura, J. Shimoyama, O. Shiino, T. Hasegawa, K. Kitazawa, and K. Kishio, Physica C **235-240**, 915 (1994).
[14] M. Marezio and F. Licci, Physica C **282**, 51 (1997).
[15] T. G. N. Babu and C. Greaves, Physica C **207**, 44 (1993).
[16] R. L. Harlow, G. H. Kwei, R. Suryanarayanan, and M. A. Subramanian, Physica C **257**, 125 (1996).
[17] L. Raffo, F. Licci, and A. Migliori, Phys. Rev. B **48**, 1192 (1993).
[18] F. Licci, G. Turilli, and P. Ferro, J. Magn. Magn. Mater. **164**, L268 (1996).
[19] P. A. Stadelmann, Ultramicroscopy **21**, 131 (1987).
[20] R. J. Cava, A. W. Hewat, E. A. Hewat, B. Batlogg, M. Marezio, K. M. Rabe, J. J. Krajewski, W. F. Peck, Jr., and L. W. Rupp, Jr., Physica C **165**, 419 (1990).
[21] F. Licci, M. Marezio, Q. Huang, and A. Santoro (unpublished).
[22] I. D. Brown, J. Solid State Chem. **90**, 155 (1991).
[23] M. François, A. Junod, K. Yvon, A. W. Hewat, J. J. Capponi, P. Strobel, M. Marezio, and P. Fischer, Solid State Commun. **66**, 1117 (1988).
[24] J. D. Jorgensen, B. W. Veal, A. P. Paulikas, L. J. Nowicki, G. W. Crabtree, H. Claus, and W. K. Kwok, Phys. Rev. B **41**, 1863 (1990).
[25] I. D. Brown, J. Solid State Chem. **82**, 122 (1989).
[26] I. D. Brown and D. Altermatt, Acta Crystallogr., Sect. B: Struct. Sci. **B41**, 244 (1985).